Soil & Tillage Research 155 (2016) 298–307

Contents lists available at ScienceDirect

Soil & Tillage Research

journal homepage: www.elsevier.com/locate/still

Depth dependence of black carbon structure, elemental and microbiological composition in anthropic Amazonian dark soil

Marcela C. Pagano[a,*], Jenaina Ribeiro-Soares[a], Luiz G. Cançado[a], Newton P.S. Falcão[b], Vívian N. Gonçalves[c], Luiz H. Rosa[c], Jacqueline A. Takahashi[d], Carlos A. Achete[e], Ado Jorio[a,*]

[a] Departamento de Física, ICEx, Universidade Federal de Minas Gerais, Avenida Antônio Carlos, 6627, Pampulha, 31.270-901 Belo Horizonte, MG, Brazil
[b] Departamento de Ciências Agronômicas, Instituto Nacional de Pesquisas da Amazônia, Manaus, 69011-970 AM, Brazil
[c] Departamento de Microbiologia, ICB, Universidade Federal de Minas Gerais, Avenida Antônio Carlos, 6627, Pampulha, 31.270-901, Belo Horizonte, MG, Brazil
[d] Departamento de Química, ICEx, Universidade Federal de Minas Gerais, Avenida Antônio Carlos, 6627, Pampulha, 31.270-901, Belo Horizonte, MG, Brazil
[e] INMETRO, Xerém, Duque de Caxias, RJ 25250-020, Brazil

ARTICLE INFO

Article history:
Received 16 June 2015
Received in revised form 28 August 2015
Accepted 1 September 2015

Keywords:
Amazonian dark soil
Soil depth
Black carbon
Microbiota
Fungi
Bacteria
Arbuscular mycorrhizas

ABSTRACT

"*Terras Pretas de Índio*" are anthropic Amazonian soils rich in pyrogenic black carbon, which might be responsible for the soil long-term stability and high fertility. This black carbon, produced by the Indians while handling their residues, became a model material for agriculture and environment. The key question to answer for artificially reproducing the desired agricultural properties of the *Terra Preta de Índio* is whether the black carbon structure found today in these soils is the same as produced by the ancient Indians, or whether its structure results from long-term complex physical, chemical and biological activities in the soil. To address this question, this work investigates the depth dependence of the properties from a soil collected from the Balbina site, in Presidente Figueiredo, Amazonas State, Brazil. The black carbon structure and the soil composition are investigated, with special emphasis on the poorly studied microbiological composition (fungi, bacteria, arbuscular mycorrhizas). The comparative analysis between the properties from shallower (newer) and deeper (older) soil strata indicates that, while soil composition exhibits depth dependence, the pyrogenic black carbon structure does not. This finding suggests that this model material should be reproducible by repeating the pyrolysis conditions utilized in their production.

1. Introduction

Understanding the characteristics of the Amazonian Dark soils "*Terras Pretas de Índio*" (TPIs) is of ecological importance, because the TPI soils represent a residue-based model for tropical sustainable agriculture (Sombroek et al., 2003; Neves et al., 2003; Cohen-Ofri et al., 2006, 2007; Falcão et al., 2003; Glaser, 2007). The TPI sites are identified by the presence of ceramics and by their deep black horizons, generally down to 1 m in depth (Fraser et al., 2011). The dark color comes from the high content of black carbon (BC), which are here defined as stable charcoal particles present in the terrestrial ecosystems (Lian et al., 2006; Liang et al., 2008). In the case of the TPI soil, the black carbon is pyrogenic, produced by the Indians when burning residues. Almost no black carbon or ceramics are detectable in immediately surrounding soils, already below 20 cm in soil depth (Glaser et al., 2001). The TPI soils sequester up to 70 times more carbon than the surrounding soils, and it is chemically and microbially stable (Glaser et al., 2001; Steiner et al., 2004). Consequently, the microbial community in the TPI is different from those in the surrounding soils (Grossman et al., 2010; Glaser and Birk, 2012).

The TPI pyrogenic black carbon (TPI-BC) is made of sp^2-ordered carbon nanocrystallites with lateral dimensions of $L_a \sim 3–8$ nm (Jorio et al., 2012; Ribeiro-Soares et al., 2013). Despite a structural complexity, the TPI-BC dimensionality (L_a) has been investigated as a critical parameter defining the stability vs. reactivity properties of the soil (Jorio et al., 2012; Ribeiro-Soares et al., 2013; Archanjo et al., 2014, 2015). To be able to reproduce charcoal structures similar to the TPI-BC, for the use as a soil conditioner, it is necessary to understand whether the TPI-BC structure (mostly L_a) found today was generated by the char and burning, or whether the time

* Corresponding authors. Fax: +55 31 3409 5600.
E-mail addresses: marpagano@gmail.com (M.C. Pagano), adojorio@fisica.ufmg.br (A. Jorio).

http://dx.doi.org/10.1016/j.still.2015.09.001
0167-1987/

exposure to complex physical, chemical and biological degradation played a role. Some authors are discussing how the microbial communities inhabiting the soil may influence its structure (Kabir et al., 1998; Oehl et al., 2005; Talbot et al., 2008; Eilers et al., 2012). While the elemental composition of the TPI has been largely studied (Glaser and Birk, 2012; Schaefer et al., 2004; Kern and Kampf, 2005; Cunha et al., 2009), few works addressed the microbiological composition (Grossman et al., 2010; Glaser and Birk, 2012).

The primary objective of this work is to detect changes in the critical parameter L_a of TPI-BC as a function of soil depth, crossing this information with the elemental and microbiological composition, from the surface down to 100 cm in depth. Estimates point to a TPI formation rate of 1 cm for every 10 years of Indian occupation (Smith, 1980). The comparative analysis among the black carbon properties from shallower (newer) and deeper (older) soil strata should provide information about the stability of their structures. The elemental composition of the soils has been measured and the microbial occurrence evaluated to test the influence of chemical elements and microorganisms as potential charcoal degradation agents. Due to the lack of information about the microbiological composition of the TPI soils, this part is discussed here in more details. The types of microorganisms present in TPI and the abundance of the associated fungi in the surface and deeper soil strata are determined. The central hypothesis of this work is that, despite differences in (1) the time permanence in the soil, (2) the elemental and (3) the microbiological soil compositions, the as produced TPI-BC maintained their basic structural properties, represented by a unique distribution of L_a values.

2. Material and methods

2.1. Samples

Individual TPI soil samples of about 0.5 kg were collected from the Balbina site, in Presidente Figueiredo (Lat. 2°09′39″S, Long 60°00′W), altitude 60 m, at 180 km from Manaus, Amazonas State, Brazil. The samples were collected in October 2011, and preserved in plastic sleeves until processed and subsampled for various biological, physical and chemical analyses. Five points within the 60 m diameter circular TPI site were selected for sampling the soil composition, as sketched in Fig. 1—four points located near the site boundaries, and one point at the central region. After removal of the litter layer, these points were probed at various depths: 0–20 cm, 20–40 cm, 40–60 cm, 60–80 cm for all sites, plus a 80–100 cm stratum for points P0, P2 and P3. Textural composition of the TPI Balbina soils is sandy, with texture independent of soil depth. The structural and microbiological analyses were performed on each sample separately, although the information presented here will be a statistical mixture among the points with same depth. For elemental analysis, however, the samples from the same depth were mixed because the amount of required material is larger for such analysis.

Control soil samples (about 0.5 kg) were collected in surrounding soils, which are predominant in the region: (1) Ultisol (USDA), under secondary rain forest vegetation or "capoeira", 30 years old, with sandy texture; (2) the immediately surrounding Oxisol, under primary forest, with a clayey texture. The ultisol and oxisol were collected at 0–20 cm and 20–40 cm strata depths only, since black carbon is not found for deeper strata. Other types of samples were analyzed for comparision, originating from: (i) native forest soil (riparian site, 0–20 cm depth) from southeastern Brazil (Sabará, Minas Gerais State, 735 m a.s.l.); (ii) turf (accumulation of decayed vegetation and other organic material), from a farm in Minas Gerais State, Brazil, from 0 to 20 cm soil depth; (iii) compost (leaves, stems, grasses and animal feces), collected from the Federal

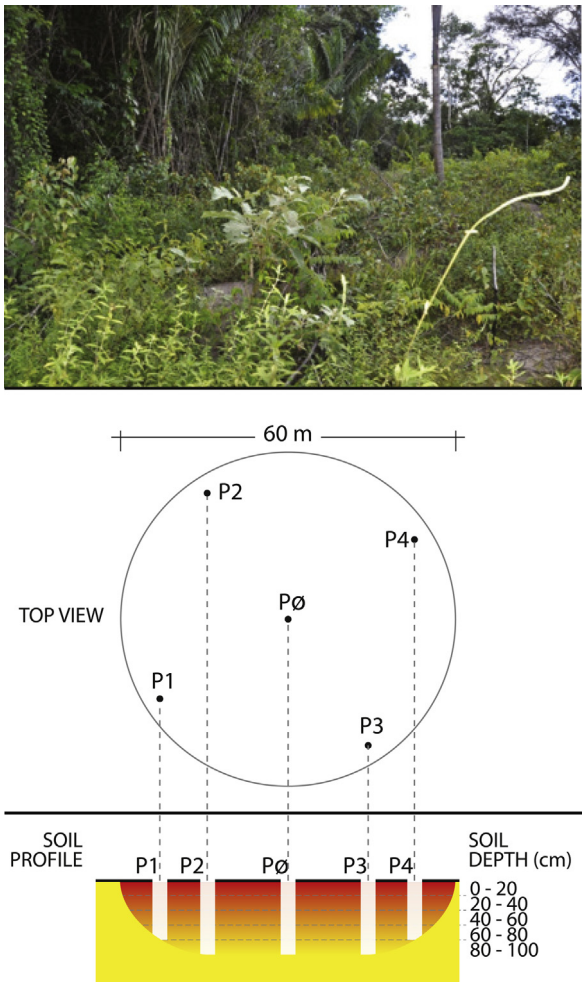

Fig. 1. Relative locations of the samples within the site of "*Terra Preta de Índio*", in Balbina, Presidente Figueiredo, Manaus State, Brazil. Five points were sampled, one in the center (P0) and four at the boundaries (P1–P4). For each point, samples were taken every 20 cm with a Dutch auger, down to 80 cm in depth for P1 and P4, and down to 100 cm in depth for the other points.

University of Minas Gerais-Campus, after 6 months of maturity; (iv) peat samples collected from the Federal University of Minas Gerais-Campus, at 7 m soil depth, during a building excavation; (v) activated charcoal (Zajac and Groszek, 1997; Suhas and Ribeiro, 2007; Qiu et al., 2008; Nabais et al., 2010), and (vi) synthetic vegetal charcoal (Schulz and Glaser, 2012), obtained from Synth® (São Paulo, Brazil).

2.2. Characterization methods

2.2.1. Elemental analysis

For elemental characterization, soil composition was obtained at Minimax® Agropecuary Laboratory, Belo Horizonte, Brazil. Phosphorus and potassium were measured according to the Mehlich I method. Organic carbon content (colorimetric method) was measured according to (EMBRAPA, 1997).

2.2.2. Structural analysis

Structural characterization of the pyrogenic TPI-BC was based on Raman spectroscopy, as discussed in Ribeiro-Soares et al. (2013). The micro-Raman scattering experiments were performed with an Andor® Tecnology-Sharmrock sr-303i spectrometer (2 cm^{-1} spectral resolution), coupled to a charge-coupled device (CCD) detector. The backscattering configuration was used, with a

60× objective lens in a Nikon Eclipse Ti-U inverted microscope. The samples were excited by a 561 nm diode laser from Coherent, with 120 μW power at the samples.

For sample preparation, after dissolution of 0.15 g soil in 1 mL ultrapure water from a Direct-Q3 system (18.2 MΩ cm, Millipore, Billerica, MA, USA), approximately 60 μL of the solution was placed onto an individual cover slip, and let dry at ambient conditions.

Thirty Raman spectra of randomly selected black carbon grains of each TPI sample were acquired. Considering five points and the different soil depths, a total of 690 spectra were analyzed. For statistical analysis based on spectral line fitting, all spectra were submitted to a linear baseline removal, between 800 cm^{-1} and 1900 cm^{-1}, and the black carbon in-plane sp^2-ordered nanocrystallite sizes (L_a) were calculated from the spectral lineshape, according to Ribeiro-Soares et al. (2013), using OriginPro 8 (SRD 2007 Origin Lab Corporation®, USA). Comparison between groups based on the obtained values for L_a was performed using Kruskal–Wallis test on MINITAB® Release 14.12.0. To support the spectral lineshape fitting analysis, Principal Component Analysis (PCA) was also used to classify the 690 TPI-BC Raman spectra, after clipping the data from 900 cm^{-1} to 1900 cm^{-1}.

2.2.3. Microbiological analysis

Because only few studies address the microbiological composition of TPI (Grossman et al., 2010; Glaser and Birk, 2012), this subsection will be more detailed.

The abundance of bacteria and total fungal microbial communities were obtained using culturing techniques. A soil sample (1 g) was diluted in water (10 mL) and mixed with a vortex shaker. The dilute (100 μL) was taken using a sterile pipette and mixed in Sterile, Potato Dextrose Agar (Himedia®) (45 °C), and then placed in the center of a sterile Petri dish (100 mm diameter). The mixture was allowed to cool and incubated at ambient conditions for 2 days or more. After this period, the colonies in the medium were counted to determine the microbial abundance, according to Hurst (2007). Original taxonomic papers based on cultural and morphological features, as well as the work by Domsch et al. (2007), were used to identify sporulating selected fungi. Single colonies were transferred to Potato Dextrose Agar and subcultured to a new MEA (malt, yeast extract and agar) plate, to obtain a pure culture and long-term stocks, prepared in 15% glycerol, and stored at −80 °C in sterilized C and in sterilized water, at Culture Collection of Microorganisms and Cells of UFMG, under the code UFMGCB.

For filamentous fungi identification, the protocol for DNA extraction followed Rosa et al. (2009). The internal transcribed spacer (ITS) region was amplified with the universal primers ITS1 and ITS4 (White et al., 1990). Amplification of the β-tubulin gene was performed with the Bt2a and Bt2b primers (Glass and Donaldson, 1995). Polymerase chain reaction (PCR) assays were conducted in 50 μL reaction mixtures containing 1 μL of genomic DNA (10 ng μL^{-1}), 5 μL of PCR buffer (100 mM Tris–HCl, 500 mM KCl, pH 8.8), 2 μL of dNTPs (10 mM) plus 3 μL of $MgCl_2$ (25 mM), 1 μL of each primer (50 pmol μL^{-1}), 1 μL of dimethyl sulfoxide (DMSO, Merck, USA), 2 μL betaine (5 M), 0.2 μL of Taq polymerase (5 U μL^{-1} DNA) and 33.8 μL of ultrapure sterile water. PCR amplifications were performed with the Mastercycler pro (Eppendorf, Hamburg, Germany), programmed for initial denaturation at 94 °C for 5 min, followed by 35 cycles of 1 min of denaturation at 94 °C, primer annealing for 1 min at 59 °C, and extension for 1.3 min at 72 °C, with a final 7 min elongation step at 72 °C. After amplification of the β-tubulin template, excess primers and dNTPs were removed from the reaction mixture using a commercial GFX column with the PCR DNA purification kit (Amersham Bioscience, Roosendaal, Netherlands). Purified PCR fragments were resuspended in 50 μL of TE buffer.

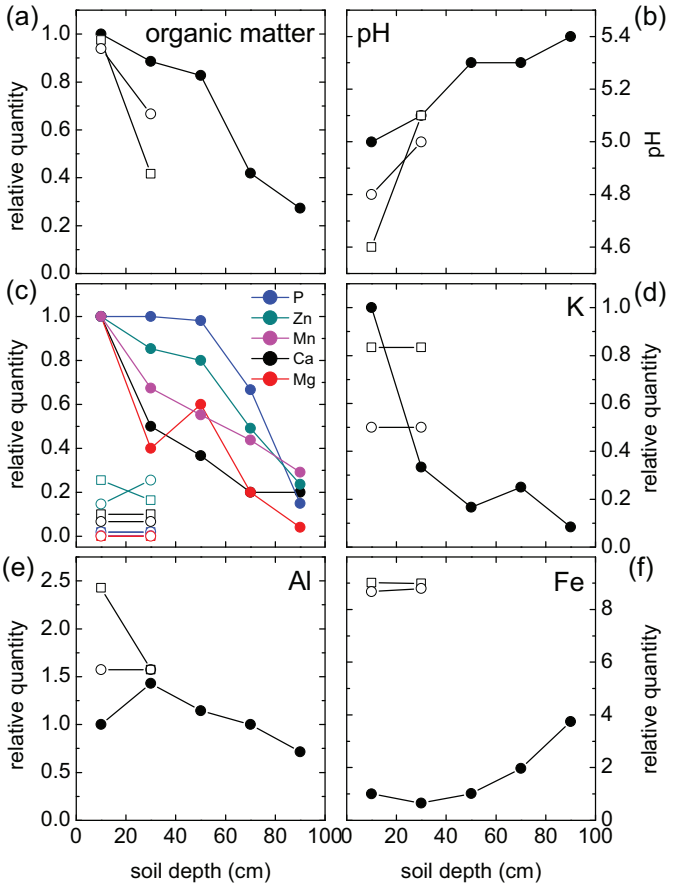

Fig. 2. Soil depth evolution for the relative elemental quantities (see figure legend) found in the "*Terra Preta de Índio*" (filled data) and control soils (open circles for ultisol and open squares for oxisol). All data values are normalized to the respective elemental quantities found in the shallower (0–20 cm) sample of the TPI site.

Table 1
Chemical properties of (a) "*Terra Preta de Índio”* (TPI)[a] and (b) adjacent soils, for different soil depths.

(a)	TPI Soil depth				
	0–20 cm	20–40 cm	40–60 cm	60–80 cm	80–100 cm
pH (H_2O)	5.0	5.1	5.3	5.3	5.4
C (g kg^{-1})	16.2	14.3	13.4	6.8	4.4
Ca (cmolc kg^{-1})	3	1.5	1.1	0.6	0.6
Mg (cmolc kg^{-1})	0.5	0.2	0.3	0.1	0.02
Al (cmolc kg^{-1})	0.7	1	0.8	0.7	0.5
K (mg kg^{-1})	12	4	2	3	1
P (mg kg^{-1})	54	54	53	36	8
Fe (mg kg^{-1})	36.5	24	37	72	136.8
Zn (mg kg^{-1})	5.5	4.7	4.4	2.7	1.3
Mn (mg kg^{-1})	64.6	43.5	35.7	28.3	18.8

(b)	Ultisol		Oxisol	
	0–20 cm	20–40 cm	0–20 cm	20–40 cm
pH (H_2O)	4.6	5.1	4.8	5.0
C (g kg^{-1})	15.8	6.7	15.2	10.8
Ca (cmolc kg^{-1})	0.3	0.3	0.2	0.2
Mg (cmolc kg^{-1})	0.0	0.0	0.0	0.0
Al (cmolc kg^{-1})	1.7	1.1	1.1	1.1
K (mg kg^{-1})	10	10	6	6
P (mg kg^{-1})	1	1	1	1
Fe (mg kg^{-1})	329	328	316.6	321.2
Zn (mg kg^{-1})	1.4	0.9	0.8	1.4
Mn (mg kg^{-1})	0.1	0.1	0.1	0.1

[a] Analyzed samples are mixtures of the samples from the five points (P0–P4) from the same soil depth.

The amplified DNA was concentrated and purified using the Wizard Plus SV Miniprep DNA Purification System (Promega, USA), and sequenced using an ET Dynamic Terminator Kit in a MegaBACE™ 1000/Automated 96Capillary DNA sequencer (GE Healthcar, USA). The obtained sequences were analysed with SeqMan Π using Lasergene software (DNASTAR/Inc.), and a consensus sequence was obtained using the Bioedit v. 7.0.5.3 software. To achieve species-rank identification based on ITS and β-tubulin data, the consensus sequence was aligned with all sequences from related species retrieved from the NCBI GenBank database using BLAST (Altschul et al., 1997). The consensus sequences of the fungi were deposited into GenBank. However, according to Gazis et al. (2011), sequencing of the ITS region may fail to recognize some fungal genera. For this reason, the β-tubulin sequences, which are considered promising for a one-gene phylogeny (Frisvad and Samson, 2004), were used to elucidate the taxonomic positions of the inconclusive taxa identified using ITS sequences. Additionally, the following criteria were used to interpret the sequences from the GenBank database: for query coverage and sequence identities ≥99%, the genus and species were accepted; for query coverage and sequence identities showing 98%, the genus and species were accepted, but the term 'cf.' (Latin for confer = compares with), used to indicate that the specimen resembles, but has certain minor features not found in the reference species, was included; for query coverage and sequence identities between 95% and 97%, only the genus was accepted; for query coverage and sequence identities ≤95%, the isolates were labelled with the order or family name, or as 'unknown' fungi. Furthermore, taxa that displayed query coverage and identities ≤97% or an inconclusive taxonomic position were subjected to phylogenetic ITS and β-tubulin analysis, with estimations conducted using MEGA Version 5.0 (Tamura et al., 2011). The maximum composite likelihood method was employed to estimate evolutionary distances with bootstrap values calculated from 1000 replicate runs. To complete the molecular identification, the sequences of known-type fungal strains or reference sequences obtained from fungal species deposited in international Culture Collections found in GenBank were added to improve the accuracy of the phylogenetic analysis. The information about fungal taxonomic hierarchical follows the rules established by (Kirk et al., 2008) and the MycoBank (www.mycobank.org), and the Index Fungorum databases (www.indexfungorum.org).

The abundance of arbuscular mycorrhizas was measured based on morphological methods. Arbuscular mycorrhizal fungi (AMF) spores were recovered from five soil samples (20 g), from each depth strata, from each of the five points of the TPI soil, and from the four control soil samples (oxisol and ultisol at two depths). Spores were separated by wet sieving (Gerdemann and Nicolson, 1963) decanting and sucrose centrifugation (Walker et al., 1982), and the analysed data were expressed as number of spores/20 g of dry soil. Only healthy spores were counted. Each spore type was mounted sequentially in polyvinyl-lacto-glycerol (PVLG) and Melzer's reagent for identification. Identification was based on spore color, size, surface ornamentation and wall structure, with reference to the descriptions provided by the original species descriptions. AMF nomenclature and authorities are those of IMA fungus (Oehl et al., 2011) and mycobank (www.mycobank.org). Numbers of species were counted and spore numbers were square rooted transformed and statistically analyzed. We estimated the AMF diversity by the Shannon index using the PAST version 2.17b software (Hammer et al., 2001). The Shannon–Weaver index (H') was calculated from the equation $H = -\sum pi \ln pi$, where pi is the relative abundance of the species compared to all the species in a sample.

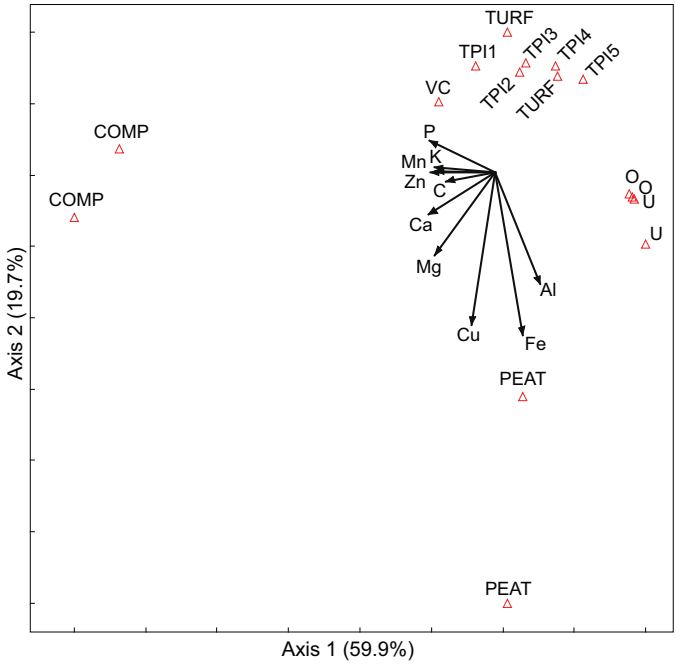

Fig. 3. PCA ordination diagram for the elemental composition of the TPI soil and other related materials. The samples are abbreviated as: TPI1 = TPI from 0 to 20 cm, TPI2 = TPI from 20 to 40 cm; TPI3 = TPI from 40 to 60 cm; TPI4 = TPI from 60 to 80 cm; TPI5 = TPI from 80 to 100 cm; TURF = turf (from 0 to 20 cm); PEAT = peat (from 7 m); COMP = compost; O = oxisols; U = ultisols; VC = synthetic vegetal charcoal.

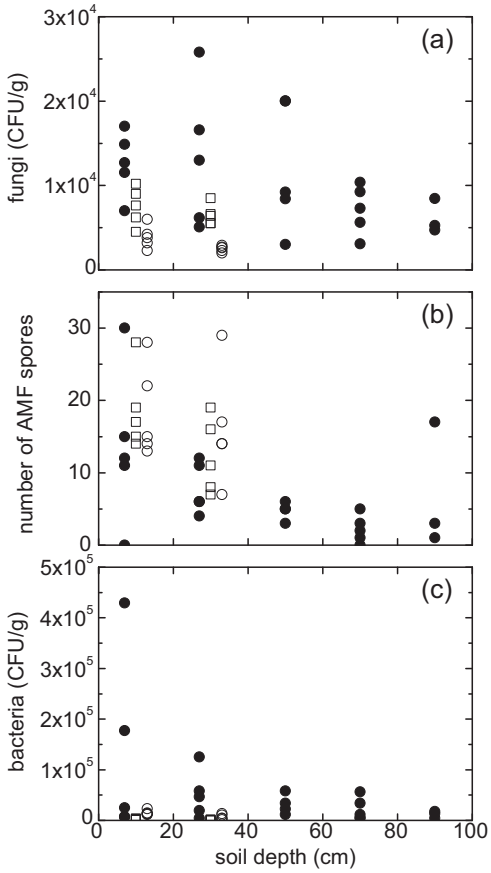

Fig. 4. Populations of (a) culturable fungi, (b) arbuscular mycorrhizal fungi (AMF) and (c) bacteria, as a function of soil depth. Solid data stand for the "*Terra Preta de Índio*", open circles and open squares stand for the control samples, ultisol and oxisol, respectively.

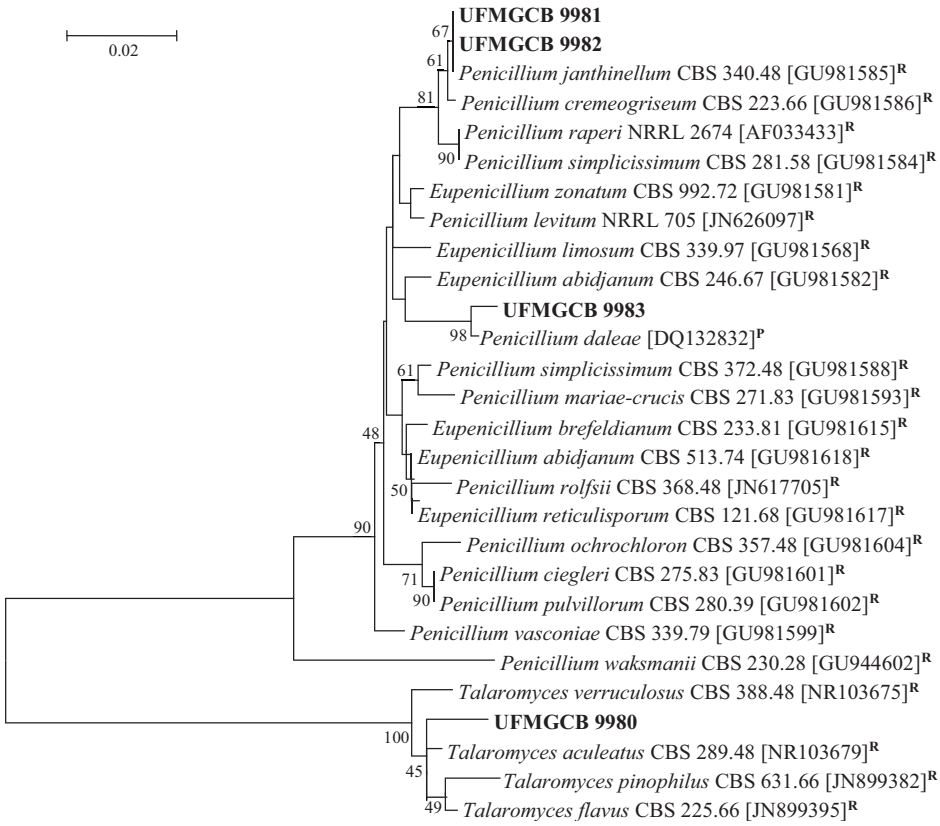

Fig. 5. Phylogenetic analysis of the fungi sequences (in bold) associated with "*Terra Preta de Índio*" samples, in comparison with reference (**R** superscript) sequences of the closest species, following BLAST analysis, deposited in the GenBank database. The tree was constructed based on the ITS region sequences using the maximum composite likelihood method.

For the statistical analysis, different methods were used. Cluster analysis was carried out with the PAST version 2.17b software (Hammer et al., 2001) to generate dendrograms using the unweighted pair-group method, with arithmetic average (UPGMA) and Euclidean distance as similarity measure. Principal component analysis (PCA) was applied to demonstrate the ordination of the AMF species from the five soil depths and to identify which soil attributes were related with the AMF species. The chemical attributes of soil, and the most commonly found AMF species were transformed into ordinates corresponding to their projection on the ordination axes, or eigenvalues, representing the weight of each variable on each component (axis) and with a correlation coefficient ranging from −1 to +1. These analyses were performed with the PC-ORD Version 5.17 Software, Gleneden Beach, Oregon, U.S.A. (McCune and Mefford, 2006).

3. Results and discussion

3.1. Elemental analysis

The amounts of organic matter, nutrients (P, Zn, Mn, Ca, Mg, K, Al, Fe, B and Cu), and the $pH_{(H_2O)}$ were measured as a function of soil depth (see Table 1). Fig. 2 shows the variation of the relative elemental quantity with soil depth, found in the TPI (filled data) and control soils (ultisol—open circles, and oxisol—open squares). The data are normalized to the respective values found at the TPI soil surface (0–20 cm).

Percent soil organic matter, directly related to the abundance of N and C, vary with depth, deeply decreasing from 60 to 100 cm in the TPI, as shown in Fig. 2(a). The decrease in organic matter relative quantity for both TPI and control soils correlate with the increase in the $pH_{(H_2O)}$, as shown in Fig. 2(b). The macronutrients

Table 2
Molecular identification of fungi isolated from "*Terra Preta de Índio*".

UFMGCB[a]	Top BLAST search results [GenBank accession no.]	Query cover (%)	Identity (%)	No. of DNA base pair analyzed	Proposed taxa [GenBank acc. no.]
9980[b]	*Talaromyces verruculosus* [HQ607919]	100	99	467	[d]*Talaromyces verruculosus* [KF926645[e]]
9981[b]	*Penicillium aculeatum* [JN166804]	100	100	489	[d]*Penicillium janthinellum* [KF926646[e]]
9982[b]	*Penicillium aculeatum* [JN166804]	100	100	463	[d]*Penicillium* sp. [KF926647[e]]
9983[b,c]	*Penicillium dalea* [JQ776541]	100	100	458	[d]*Eupenicillium* sp. [KF926648[e], KJ473427[f]]

Identification conducted using BLASTn searches of the internal transcribed spacer (ITS) and β-tubulin gene regions. [a]UFMGCB = Culture of Microorganisms and Cells from the Federal University of Minas Gerais. Taxa subjected to phylogenetic analysis based on the [b]ITS and [c]β-tubulin regions for elucidation of taxonomic positions. [d]Taxonomic position suggested by the phylogenetic analyses. [e]ITS and [f]β-tubulin sequences deposited.

Table 3
Top five BLAST results identifying the sequences of fungi from "*Terra Preta de Índio*" samples, and their habitat.

UFMGCB[a]	Closest relative taxa [GenBank accession no.]	Maximal identity (%)	Query coverage (%)	Originally reported habitat
9980	*Talaromyces verruculosus* [HQ607919]	99	100	Associated with fungus-gardens of a lower-attine ant *Cyphomyrmex wheeleri*, USA (Rodrigues et al., 2011)
	Penicillium pinophilum [AY753344]	99	100	Unknown, Thailand
	Fungal endophyte [KF673656]	99	100	Fungal endophytes of aquatic macrophytes, USA
	Fungal sp. [KC506174]	99	100	Mangroves sediments, Brazil
	Penicillium aculeatum [GU566285.1]	99	100	*Phalaris arundinacea* L. in field experiment on a coal mine spoil bank Czech Republic (Bukovska et al., 2010)
9981	*Penicillium aculeatum* [JN166804]	100	100	Unknown, China
	Penicillium janthinellum [FJ004303]	100	100	Unknown, Greece
	Cladosporium sp.[GQ370370]	100	100	Endophytic and rhizosphere fungi isolated from sugarcane, Brazil (Rojas et al., 2012)
	Penicillium janthinellum [GU981585]	100	100	Leaf litter, The Netherlands (Houbraken et al., 2011)
	Penicillium cremeogriseum [JX091428]	99	100	Unknown, South Africa
9982	*Penicillium aculeatum* [JN166804]	100	100	Unknown, China
	Penicillium janthinellum [FJ004303]	100	100	Unknown, Greece
	Cladosporium sp.[GQ370370]	100	100	Endophytic and rhizosphere fungi isolated from sugarcane, Brazil (Rojas et al., 2012)
	Penicillium cremeogriseum [JX091428]	99	100	Unknown, South Africa
	Penicillium ochrochloron [HQ392499]	99	100	Microfungi from freshwater ecosystem, Malaysia
9983	*Paecilomyces parvisporus* [JQ776543]	100	100	Endophytic fungi from *Cymodocea rotundata*, tropical seagrass leaves, India
	Penicillium dalea [JQ776541]	100	100	Endophytic fungi from *Cymodocea rotundata*, tropical seagrass leaves, India
	Penicillium daleae [DQ132832]	99	99	Rhizosphere of clonal *Picea mariana*, Canada (Vujanovic et al., 2007)
	Paecilomyces parvisporus [DQ187954]	99	99	Soil samples of Dali City, China (Han et al., 2005)
	Penicillium daleae [KF156321]	96	99	Root associated fungi of healthy-looking *Pinus sylvestris* and *Picea abies* seedlings, Swedish forest nurseries

[a] UFMGCB = culture of microorganisms and cells from the Federal University of Minas Gerais.

(P, Ca and Mg) and micronutrients (Zn and Mn) are much more abundant in the TPI than in the control soils, and decrease significantly with depth (Fig. 2(c)). The P level is high down to 60 cm, decreasing sharply after 80 cm. Differently, the amount of K (Fig. 2(d)) is not much higher in the TPI as compared to the control soils, and it decreases quickly with increasing soil depth, indicating it has a stronger dependence on the soil surface composition; the absolute value of K contents was low anyways (see Table 1). For B and Cu (not shown), only traces were found. The absolute amounts of exchangeable Al (Fig. 2(e)) are very low at all soil depths, consistent with the $pH_{(H_2O)}$ values. The slight decrease of these values with depth may be correlated with the slight increase of pH with depth. The Fe content (Fig. 2(f)) in the control soils was much higher than in the TPI. In general, Fe content is low in TPI soils.

Fig. 3 shows a PCA ordination diagram for the elemental composition of the PTI soils and other related materials (peat, turf, compost, control soils: oxisol and utisol, and synthetic vegetal charcoal—see Section 2.1). When comparing the elemental composition on the TPI soil with the other samples, the level of available nutrients follow the order compost > TPI > peat > turf > synthetic vegetal charcoal > control soils, although exceptions are found for specific elements, such as K and Cu, which exhibit elevated levels in peat. These findings agree with the association between charcoal and composting by the natives, who incorporated organic wastes such as mammalian and fish bones (Lima et al., 2002; Schaefer et al., 2004).

3.2. Microbial analysis

Microbiological analyses show that the "*Terra Preta de Índio*" soil contains high microbial abundance and diversity. These composition aspects are described here in details due to the lack of information in the literature about the microbiological composition of the TPI.

Fig. 4 plots the soil depth dependence for the population of culturable fungi, arbuscular mycorrhizal fungi (AMF) and bacteria, in the TPI (filled symbols) and control soils (open circles—ultisol; open squares—oxisol). Abundance of culturable fungi, AMF and bacteria decreases with increasing depth. The greater fungi CFU (colony-forming units) recovery in the TPI soils may reflect the natural variability in the soils or may simply reflect the enhanced culturability of the fungi on taxa-specific media, as compared to general purpose media. Despite certain well-known limitations of plate cultivation techniques, the CFU results independently indicate that the fungi are naturally elevated in the TPI soil and decrease with depth (Fig. 4). Remarkable is the much higher content of bacteria in the TPI as compared to the control soils.

For fungal species identification, molecular and morphological analysis was performed. In the molecular analysis, the Phylum Ascomycota predominated. The internal transcribed spacer (ITS) sequence from the TPI soils was compared with sequences from the species deposited in the GenBank database (details in Fig. 5). Four isolated fungi were identified, as listed in Table 2. As the ITS region from terverticillate *Penicillia* alone cannot differentiate *Penicillium* species (Skouboe et al., 2000), the β-tubulin gene (Seifert and Louis-Seize, 2000) was also analyzed for classifying

Table 4
Distribution of AMF species in the TPI and control soils—oxisol and utisol, in the different depths (+, presence; –, absence).

AMF species	TPI[a]					Control soils[a]	
	0–20	20–40	40–60	60–80	80–100	0–20	20–40
Acaulosporaceae							
Acaulospora bireticulata F.M. Rothwell & Trappe	+	–	+	–	–	–	–
A. sp.1	–	–	–	+	–	–	–
A. mellea Spain & Schenck	+	+	+	+	–	–	+
A. rhemii Sieverding & Toro	+	–	+	–	+	–	–
A. scrobiculata Trappe	+	+	+	+	+	–	–
A. spinosa C. Walker & Trappe	–	–	–	–	+	–	+
Ambisporaceae							
Ambispora appendicula (Spain, Sieverd. & N.C. Schenck) C. Walker	+	–	–	–	–	–	–
Entrophosporaceae							
Claroideoglomus etunicatum (W.N. Becker & Gerd.) C. Walker & A. Schüβler	+	+	+	+	+	+	+
Scutellosporaceae							
Scutellospora calospora (T.H. Nicolson & Gerd.) C. Walker & F.E. Sanders	–	–	–	+	+	+	+
Racocetra castanea (C. Walker) Oehl, F.A.Souza & Sieverd.	–	–	–	–	–	+	–
Glomeraceae							
Funneliformes geosporus (T.H. Nicolson & Gerd.) C. Walker & Schüβler	+	+	+	+	+	+	–
Glomus tortuosum N.C. Schenck & G.S. Smith	–	–	–	–	-	-	+
Glomus rubiforme (Gerd. & Trappe) R.T. Almeida & N.C. Schenck	+	–	–	–	–	–	+
Glomus sp. 1	+	+	+	–	–	–	–
Glomus sp. 2	+	+	–	–	–	–	–
Glomus sp. 3	+	+	–	+	+	–	+
Glomus sp. 4	–	–	+	+	–	+	–
Glomus sp. 5	–	–	+	+	–	+	–
Pacisporaceae							
Pacispora franciscana Sieverd. & Oehl	+	+	+	+	–	–	–
Species richness (number of species)	12	8	9	10	7	6	7
Diversity[b]	1.8	1.8	1.8	1.8	1.8	1.1	1.8

[a] Data obtained for each soil depth: 0–20 = 0–20 cm; 20–40 = 20–40 cm, and so on.
[b] Maximal AMF diversity using the Shannon index.

one isolate from TPI. In this analysis, the isolate was 100% identical to the *P. daleae* (JQ776541) species. Molecular analysis suggests that isolates assigned to genera *Talaromyces verruculosus*, *Penicillium janthinellum* and *Eupenicillium* sp. (Trichocomaceae) can be found in the TPI soils, in all soil depths.

All the filamentous fungi found in the present work match with fungi previously associated with C sources, which were found generally in the rhizosphere soil as plant endophytic, or associated to leaf litter (Table 3). Among them, *T. verruculosus* was found associated with fungus-gardens of a lower-attine ant *Cyphomyrmex wheeleri* (Rodrigues et al., 2011). *P. janthinellum* is a soil fungi previously isolated in Amazonia (Batista et al., 1967a,b) that can also live as an endophyte (Khan et al., 2013). It was also isolated from humic and ferulic acids being able to decompose starch, cellulose, tannins and hydrocarbons from fuel oil (Domsch et al., 2007).

In the morphological analysis of arbuscular mycorrhizas, we identified 11 AMF species, and 6 were unidentified (only gender was known) (Table 4 and Fig. 6). Glomeromycota were dominated by Diversisporales, followed by Glomerales and Gigasporales. Previous observations showed that most of the AMF species richness (number of different species) and diversity (Shannon index) are concentrated in the topmost soil horizons (Oehl et al., 2005), consistent with our data. The *Scutellospora* species was found only in the deeper strata, in agreement with Oehl et al. (2005). Richness estimators showed a declining trend with increasing depth; however, diversity remained similar (see Table 4).

With regard to the control soil samples (oxisol and utisol), similar AMF species were detected, with 8 AMF species identified

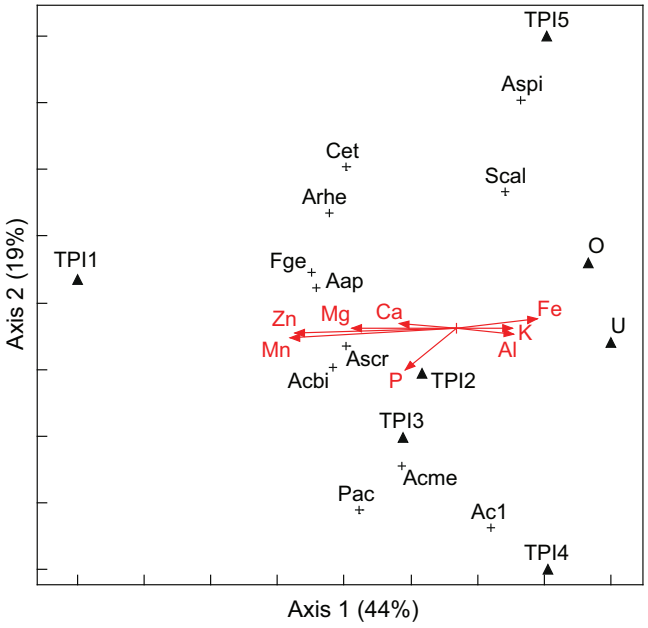

Fig. 6. PCA AMF ordination diagram for the five different TPI soil depths and control soils. Samples abbreviations: TPI1 = TPI from 0 to 20 cm, TPI2 = TPI from 20 to 40 cm; TPI3 = TPI from 40 to 60 cm; TPI4 = TPI from 60 to 80 cm; TPI5 = TPI from 80 to 100 cm; O = oxisols; U = ultisols. AMF species abbreviations: Aap = *Ambispora appendicula*; Arhe = *A. rhemii*; Ascr = *A. scrobiculata*; Ac1 = *Acaulospora* sp.1; Acbir = *Acaulospora bireticulata*; Acme = *Acaulospora mellea*; Aspi = *A. spinosa;* Scal = *Scutellospora calospora*; Cet = *Claroideoglomus etunicatum*; Fgeo = *Funneliformes geosporus*; Pac = *Pacispora franciscana*. Elemental ordination is also added.

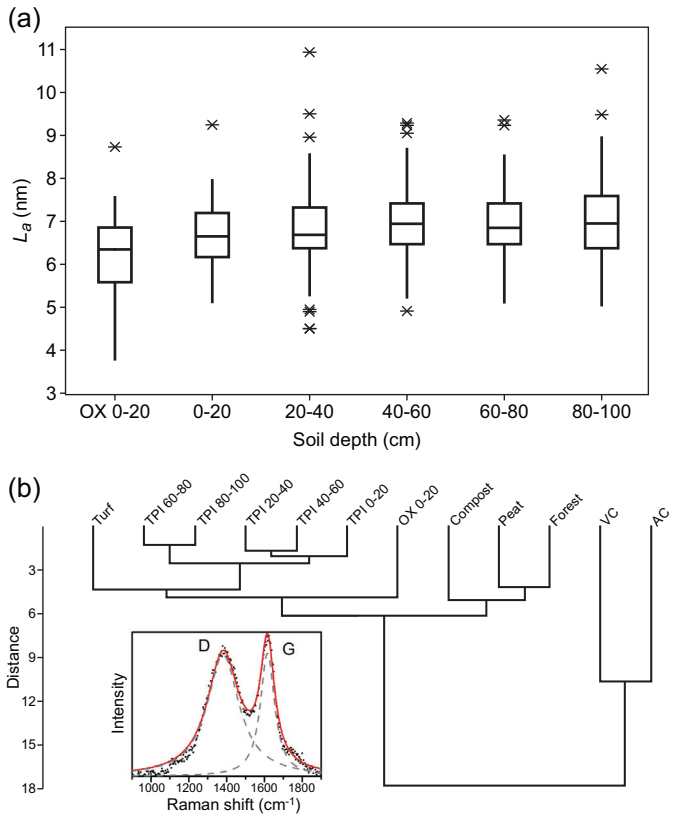

Fig. 7. (a) Box-plot representation of the average crystallite size L_a of black carbon present in the "*Terra Preta de Índio*" at each soil depth. The first data on the left stands for the control soil (labeled OX 0–20 in the *X*-axis). The line inside the boxes give the median values. Boundaries of the boxes indicate the 25th and 75th percentiles, respectively. The remaining data are in the range delimited by the horizontal lines outside the boxes, while outliers are represented as asterisks. (b) Dendrogram constructed by UPGMA using the crystallite size (L_a, nm) of TPI-BC at each depth, and the reference samples—abbreviations: VC = synthetic vegetal charcoal; AC = activated charcoal, OX 0–20 = adjacent oxisol (0–20 cm). The inset shows a Raman spectrum of a TPI-BC sample (from the 40 to 60 cm soil depth stratum). The D and G Raman lines are labeled.

and 3 unidentified. However, *Racocetra castanea* was found in the control soil only at 0–20 cm. In the Amazon region (Maranhão, Brazil), 16 AMF species, belonging to *Acaulospora*, *Ambispora*, *Glomus, Gigaspora* and *Scutellospora* were found in alley cropping system with legume trees (Nobre et al., 2010). Among them, six species were in common with the present survey. Recently, Freitas et al. (2014) found in a protected area near Manaus, Amazonas, higher species richness (39 AMF species); however, they analyzed 102 soil samples (in a bigger sampled area). Only nine species were in common with the present study, but the number of AMF taxa might be underestimated here due to the restricted sampling. The microbiological analysis showed that the abundance of AMF was greater in TPI > control soil > turf samples. Peat was collected from 7 m depth and did not present any AMF, while compost presented few *Glomus* spores (data not shown).

3.3. Structural analysis

Fig. 7(a and b) brings the structural analysis of the TPI-BC based on Raman spectroscopy, as previously discussed (Jorio and Cançado, 2012; Jorio et al., 2012; Ribeiro-Soares et al., 2013). The main structural parameter is the in-plane crystallite size (L_a) for the sp^2 coordinated carbons. The inset in Fig. 7(b) shows a representative Raman spectrum, which reveals the presence of the D (~1376 cm^{-1}) and G (~1610 cm^{-1}) Raman lines, obtained from a TPI-BC grain in the 40–60 cm deep stratum.

Statistical analysis of the measured TPI-BC Raman spectra indicates an average crystallite size (L_a) ranging mostly from $\sim 4 < L_a < \sim 9$ nm, with average L_a value of 6.8 nm (Fig. 7(a)). These findings agree with previous works showing $L_a \sim 3$–8 nm for TPI-BC-grains (Jorio et al., 2012; Ribeiro-Soares et al., 2013). Comparing results from the TPI-BC with results from turf and synthetic vegetal charcoal, the L_a from TPI-BC is similar to turf (~6 nm) and lower than that of synthetic vegetal charcoal (~10 nm), also consistent with previous findings (Jorio et al., 2012). A slightly lower mean value of L_a (6.3 nm) was found for the control soil (oxisol, 0–20 cm) as compared to the results from the TPI-BC (6.7 nm) at the same 0–20 cm depth (Table 5). Other reports of Raman spectra from fossil charcoal showed similar crystallite size (Cohen-Ofri et al., 2006).

Fig. 7(b) clusters the samples of different origins and depths according to their nanocrystallite sizes (L_a), as obtained by Raman spectroscopy analysis. The analysis revealed the formation of two main clusters: the first cluster includes synthetic samples of vegetal charcoal and activated charcoal, and the second cluster includes the non-synthetic samples. The compost samples are considered here of natural origin, since they are the stable product of controlled microbial aerobic decomposition and stabilization of organic substrates (Martin et al., 2012). PCA was also performed in the raw data, analyzing the 690 Raman spectra from the TPI. The formation of data grouping could not be obtained.

Therefore, although the Raman spectroscopy analysis is able to sort out the carbon structures found in different sources, the properties did not vary significantly among the TPI soil strata (Fig. 7(a)). This means that, although oxidation (or degradation) of the TPI-BC could increase over time, the Raman spectroscopy analysis does not evidence any indication of structural changes from the surface layers as compared to the deeper TPI samples.

4. Conclusions

Raman spectroscopy-based structural analysis is capable of realizing the differences among black carbon structures from TPI, turf, peat, compost, nature forest, synthetic vegetal and activated

Table 5
Depth dependence for the average crystallite size L_a and the widths and positions of the D and G peaks of black carbon from "*Terra Preta de Índio*" and the oxisol control soil. Medians followed by different lowercase letters in a column indicate significant differences, as determined by *t*-Student test at the 5% significance level. Same uppercase letters in each column indicate no significantly differences between soil depths ($P < 0.05$).

Soil type	Soil depth (cm)	L_a (nm)	Width D (cm^{-1})	Width G (cm^{-1})	Peak D (cm^{-1})	Peak G (cm^{-1})
TPI	0–20	6.65† Aa	205.62 Aa	88.48 Aa	1385.2 Aa	1619.1 Aa
	20–40	6.70† AB	200.36 B	88.00 A	1384.4 A	1618.6 A
	40–60	6.98† B	187.39C	85.04 B	1384.5 A	1619.6 AB
	60–80	6.85† B	191.90C	86.32 B	1384.8 A	1619.9 AB
	80–100	6.95‡ B	186.49C	85.30 B	1384 A	1619.6 AB
Oxisol	0–20	6.34* b	229.85 b	93.75 b	1361.7 b	1593.9 b

For L_a, medians are taken from †150, ‡90, *30 measurements.

commercial charcoals. However, the Raman spectroscopy analysis indicates that the nanostructure parameter L_a of the TPI-BC does not change with soil depth. On the other side, the elemental composition and the microbial abundance were found to exhibit a clear depth dependence. Based on these results, we propose that the nanostructure of the TPI-BC found today is similar to the form they were produced by the Indians, i.e. they have not experienced long-term degradation. This is a key aspect to synthesize this type of black carbon structure, since it suggests one has to reproduce the conditions utilized by the Indians, excluding complex unknown long-term physical–chemical–biological influences on the TPI-BC structure in the soil.

From materials science, it is known that the differences in the annealing temperature is the main factor that mostly influences L_a (Takai et al., 2003; Cançado et al., 2006). In analogy, controlling the pyrolysis temperature and atmosphere during residues burning might be a key aspect to reproduce the TPI-BC nanostructure.

Conflict of interest

The authors declare no conflict of interest.

Author contributions

MCP conducted all the experimental work and analysis. JRS and LGC helped with the Raman spectroscopy experiments and analysis. NPSF, CAA and AJ collected the TPI samples. VNG, LHR and JAT, helped with microbiological analysis. MCP and AJ idealized and conducted the project. The manuscript was written by MCP and AJ, with contributions from all the authors.

Funding sources

CAPES-PNPD (Process no. 23038.007147/2011-60), CNPq (Grant no. 473840/2012-0), Fundação de Amparo a Pesquisa do Estado de Minas Gerais (FAPEMIG), Fundação de Amparo a Pesquisa do Estado do Amazonas (FAPEAM), and Fundação de Amparo a Pesquisa do Estado do Rio de Janeiro (FAPERJ).

Acknowledgements

The authors acknowledge Cassiano Rabelo e Silva for technical assistance. This work was supported by CAPES-PNPD (grant no. 23038.007147/2011-60) and CNPq (grant no. 473840/2012-0). We also acknowledge financial support from the State Agencies of Minas Gerais (FAPEMIG), Amazonas (FAPEAM) and Rio de Janeiro (FAPERJ).

References

Archanjo, B.S., Araujo, J.R., Silva, A.M., Capaz, R.B., Falcão, N.P.S., Jorio, A., Achete, C.A., 2014. Chemical analysis and molecular models for calcium–oxygen–carbon interactions in black carbon found in fertile Amazonian anthrosoils. Environ. Sci. Technol. 48, 7445–7452.

Archanjo, B.S., Baptista, D.L., Sena, L.A., Cançado, L.G., Falcao, N.P.S., Jorio, A., Achete, C.A., 2015. Nanoscale mapping of carbon oxidation in pyrogenic black carbon from ancient Amazonian anthrosols. Environ. Sci. Process. Impacts 17, 775.

Altschul, S.F., Madden, T.L., Schaffer, A.A., Zhang, J.H., Zhang, Z., Miller, W., Lipman, D. J., 1997. Gapped BLAST and PSI-BLAST: a new generation of protein database search programs. Nucleic Acids Res. 25, 3389–3402.

Batista, A.C., Oliveira da Silva, J., Perez Maciel, M.J., Americo de Lima, J., Ramos de Moura, N., 1967a. Micropopulações fúngicas dos solos do território federal do Amapá. Atas Instit. Micol. 4, 117–121.

Batista, A.C., Oliveira da Silva, J., Perez Maciel, M.J., Gonzaga de Almeida, A., 1967b. Aspergillaceae dos solos das zonas fisiograficas de Bragança e do Baixo Amazonas, estado do Pará. Atas Inst. Micol. 4, 185–189.

Bukovska, P., Jelinkova, M., Hrselova, H., Sykorova, Z., Gryndler, M., 2010. Terminal restriction fragment length measurement errors are affected mainly by fragment length, G + C nucleotide content and secondary structure melting point. J. Microbiol. Methods 82, 223–228.

Cançado, L.G., Takai, K., Enoki, T., Endo, M., Kim, Y.A., Mizusaki, H., Jorio, A., Coelho, L. N., Magalhães-Paniago, R., Pimenta, M.A., 2006. General equation for the determination of the crystallite size La of nanographite by Raman spectroscopy. Appl. Phys. Lett. 88, 163106.

Cohen-Ofri, I., Weiner, L., Boaretto, E., Mintz, G., Weiner, S., 2006. Modern and fossil charcoal: aspects of structure and diagenesis. J. Archaeol. Sci. 33, 428–439.

Cohen-Ofri, I., Popovitz-Biro, R., Weiner, S., 2007. Structural characterization of modern and fossilized charcoal produced in natural fires as determined by using electron energy loss spectroscopy. Chem.-Eur. J. 13, 2306–2310.

Cunha, T.J.F., Madari, B.E., Canellas, L.P., Ribeiro, L.P., Benites, V.M., Santos, G.A., 2009. Soil organic matter and fertility of anthropogenic dark earths (terra preta de Índio) in the Brazilian Amazon basin. Rev. Bras. Ciênc. Solo 33 (1), 85–93.

Domsch, K.H., Gams, W., Anderson, T., 2007. Compendium of Soil Fungi. IHW-Verlag, Eching.

Eilers, K.G., Debenport, S., Anderson, S., Fierer, N., 2012. Digging deeper to find unique microbial communities: the strong effect of depth on the structure of bacterial and archaeal communities in soil. Soil Biol. Biochem. 50, 58–65.

EMBRAPA, 1997. Manual for Methods of Soil Analysis. National Service for Soil Survey and Soil Conservation, Rio de Janeiro, Brazil.

Falcão, N.P.S., Comerford, N., Lehmann, J., 2003. Determining nutrient bioavailability of Amazonian Dark Earth soils – methodological challenges. In: Lehmann, J., Kern, D., Glaser, B., Woods, W.I. (Eds.), Amazonian Dark Earths: Origin, properties, and Management. Kluwer, Dordrecht, pp. 255–270.

Fraser, J., Teixeira, W., Falcão, N., Woods, W., Lehmann, J., Junqueira, A.B., 2011. Anthropogenic soils in the Central Amazon: from categories to a continuum. Area 43, 264–273.

Freitas, R.O., Buscardo, E., Nagy, L., Maciel, A.B.S., Carrenho, R., Luizão, R.C.C., 2014. Arbuscular mycorrhizal fungal communities along a pedo-hydrological gradient in a Central Amazonian terra firme forest. Mycorrhiza 24, 21–32.

Frisvad, J.C., Samson, R.A., 2004. Polyphasic taxonomy of *Penicillium* subgenus *Penicillium*: a guide to identification of food and air-borne terverticillate *Penicillia* and their mycotoxins. Stud. Mycol. 49, 1–174.

Gazis, R., Rehner, S., Chaverri, P., 2011. Species delimitation in fungal endophyte diversity studies and its implications in ecological and biogeographic inferences. Mol. Ecol. 20, 3001–3013.

Gerdemann, J.W., Nicolson, T.H., 1963. Spores of mycorrhizal endogone species extracted from soil by wet sieving and decanting. Trans. Br. Mycol. Soc. 84, 679–684.

Glass, N.L., Donaldson, G.C., 1995. Development of primer sets designed for use with the PCR to amplify conserved genes from filamentous ascomycetes. Appl. Environ. Microbiol. 61, 1323–1330.

Glaser, B., 2007. Prehistorically modified soils of central Amazonia: a model for sustainable agriculture in the twenty-first century. Philos. Trans. R. Soc. B: Biol. Sci. 362, 187–196.

Glaser, B., Birk, J.J., 2012. State of the scientific knowledge on properties and genesis of Anthropogenic Dark Earths in Central Amazonia (terra preta de Índio). Geochim. Cosmochim. Acta 82, 39–51.

Glaser, B., Haumaier, L., Guggenberger, B., Zech, W., 2001. The 'terra preta' phenomenon: a model for sustainable agriculture in the humid tropics. Naturwissenschaften 88, 37–41.

Grossman, J.M., O'Neill, B.E., Tsai, S.M., Liang, B., Neves, E., Lehmann, J., Thies, J.E., 2010. Amazonian anthrosols support similar microbial communities that differ distinctly from those extant in adjacent, unmodified soils of the same mineralogy. Microb. Ecol. 60, 192–205.

Hammer, O., Harper, D.A.T., Ryan, P.D., 2001. PAST: paleontological statistics software package for education and data analysis. Paleontol. Electron. 4 9. art 4, 178kb.

Han, Y., Liang, Z., Chu, H., Kang, J., 2005. Paecilomyces parvosporus, a new species with its relatives from Yunnan Province, China. Mycotaxon 94, 357–363.

Houbraken, J., Lopez-Quintero, C.A., Frisvad, J.C., Boekhout, T., Theelen, B., Franco-Molano, A.E., Samson, R.A., 2011. *Penicillium araracuarense* sp. nov., *Penicillium elleniae* sp. nov., *Penicillium penarojense* sp. nov., *Penicillium vanderhammenii* sp. nov. and *Penicillium wotroi* sp. nov., isolated from leaf litter. Int. J. Syst. Evol. Microb. 61, 1462–1475.

Hurst, C.J., 2007. Manual of Environmental Microbiology. ASM Press, Washington, D. C.

Jorio, A., Cançado, L.G., 2012. Perspectives on Raman spectroscopy of graphene-based systems: from the perfect two-dimensional surface to charcoal. Phys. Chem. Chem. Phys. 14, 15246–15256.

Kabir, Z., O'Halloran, I.P., Widden, P., Hamel, C., 1998. Vertical distribution of arbuscular mycorrhizal fungi under corn (*Zea mays* L.) in no-till and conventional tillage systems. Mycorrhiza 8, 53–55.

Jorio, A., Ribeiro-Soares, J., Cançado, L.G., Falcão, N.P.S., Dos Santos, H.F., Baptista, D. L., Martins-Ferreira, E.H., Archanjo, B.S., Achete, C.A., 2012. Microscopy and spectroscopy analysis of carbon nanostructures in highly fertile Amazonian anthrosoils. Soil Till. Res. 122, 61–66.

Kern, D.C., Kampf, N., 2005. Anthropic and pedogenic processes of Terra Preta Soils in Cachoeira-Porteira Pará State, Brazil. Boletim do Museu Paraense Emilio Goeldi serie Ciências Naturais 1, 187–201.

Khan, A.L., Waqas, M., Khan, A.R., Hussain, J., Kang, S.M., Gilani, S.A., Hamayun, M., Shin, J.H., Kamran, M., Al-Harrasi, A., Yun, B.W., Adnan, M., Lee, I.J., 2013. Fungal endophyte *Penicillium janthinellum* LK5 improves growth of ABA-deficient tomato under salinity. World J. Microbiol. Biotechnol. 29, 2133–2144.

Kirk, P.M., Cannon, P.F., Minter, D.W., Stalpers, J.A., 2008. Dictionary of the Fungi. CAB International, Wallingford, U.K.

Lian, B., Lehmann, J., Solomon, D., Kinyangi, J., Grossman, J., O'Neill, B., Skjemstad, J. O., Thies, J., Luizão, F.J., Petersen, J., Neves, E.G., 2006. Black carbon increases cation exchange capacity in soils. Soil Sci. Soc. Am. J. 70 (5), 1719–1730.
Liang, B., Lehmann, J., Solomon, D., Sohi, S., Thies, J.E., Skjemstad, J.O., Luizão, F.J., Engelhard, M.H., Neves, E.G., Wirick, S., 2008. Stability of biomass-derived black carbon in soils. Geochim. Cosmochim. Acta 72, 6069–6078.
Lima, H.N., Schaefer, C.E.R., Mello, J.W.V., Gilkes, R.J., Ker, J.C., 2002. Pedogenesis and pre-Colombian land use of terra preta anthrosols (Indian Black Earth) of Western Amazonia. Geoderma 110, 1–17.
Martin St., C.C.G., Brathwaite, R.A.I., 2012. Compost and compost tea: principles and prospects as substrates and soil-borne disease management strategies in soil-less vegetable production. Biol. Agric. Hortic. 28 (1), 1–33.
McCune, B., Mefford, M.J., 2006. PC-ORD. Multivariate Analysis of Ecological Data. Version 5.0 for Windows.
Nabais, J.M.V., Laginhas, C., Carrott, P.J.M., Ribeiro Carrott, M.M.L., 2010. Thermal conversion of a novel biomass agricultural residue (vine shoots) into activated carbon using activation with CO_2. J. Anal. Appl. Pyrolysis 87, 8–13.
Neves, E.G., Petersen, J.B., Bartone, R.N., Da Silva, C.A., 2003. Historical and socio-cultural origins of Amazonian Dark Earths. In: Lehmann, J., Kern, D., Glaser, B., Woods, W.I. (Eds.), Amazonian Dark Earths: Origin, Properties, Management. Kluwer Academic Publishers, Dodrecht, pp. 29–50.
Nobre, C.P., Ferraz, A.S.L.J., Goto, B.T., Berbara, R.L.L., Nogueira, M.D.C., 2010. Arbuscular mycorrhizal fungi in an alley cropping system in the state of Maranhão, Brazil. Acta Amazonica 40, 641–646.
Oehl, F., Sieverding, E., Ineichen, K., Ris, E.A., Boller, T., Wiemken, A., 2005. Community structure of arbuscular mycorrhizal fungi at different soil depths in extensively and intensively managed agroecosystems. New Phytol. 165, 273–283.
Oehl, F., Sieverding, E., Palenzuela, J., Ineichen, K., Silva, G.A., 2011. Advances in Glomeromycota taxonomy and classification. IMA Fungus 2, 191–199.
Qiu, Y., Cheng, H., Xu, C., Sheng, G.D., 2008. Surface characteristics of crop-residue derived black carbon and lead (II) adsorption. Water Res. 42, 567–574.
Ribeiro-Soares, J., Cançado, L.G., Falcão, N.P.S., Martins Ferreira, E.H., Achete, C.A., Jorio, A., 2013. The use of Raman spectroscopy to characterize the carbon materials found in Amazonian anthrosoils. J. Raman Spectrosc. 44, 283–289.
Rodrigues, A., Mueller, U.G., Ishak, H.D., Bacci, M., Pagnocca, F.C., 2011. Ecology of microfungal communities in gardens of fungus-growing ants (Hymenoptera: Formicidae): a year-long survey of three species of attine ants in Central Texas. FEMS Microbiol. Ecol. 78, 244–255.
Rojas, J.D., Sette, L.D., de Araujo, W.L., Lopes, M.S., da Silva, L.F., Furlan, R.L., Padilla, G., 2012. The diversity of polyketide synthase genes from sugarcane-derived fungi. Microb. Ecol. 63, 565–577.
Rosa, L.H., Vaz, A.B.M., Caligiorne, R.B., Campolina, S., Rosa, C.A., 2009. Endophytic fungi associated with the Antarctic Grass *Deschampsia antarctica* Desv. (*Poaceae*). Polar Biol. 32, 161–167.
Schaefer, C.E.G.R., Lima, H.N., Gilkes, R.J., Mello, J.W.V., 2004. Micromorphology and electron microprobe analysis of phosphorus and potassium forms of an Indian Black Earth (IBE) Anthrosol from Western Amazonia. Aust. J. Soil Res. 42, 401–409.
Schulz, H., Glaser, B., 2012. Effects of biochar compared to organic and inorganic fertilizers on soil quality and plant growth in a greenhouse experiment. J. Plant Nutr. Soil Sci. 175, 410–422.
Seifert, K.A., Louis-Seize, G., 2000. Phylogeny and species concepts in the *Penicillium aurantiogriseum* complex as inferred from partial β-tubulin gene DNA sequences. In: Samson, R.A., Pitt, J.I. (Eds.), Integration of Modern Taxonomic Methods for *Penicillium* and *Aspergillus* Classification. Harwood Academic Publishers, Netherlands, pp. 189–198.
Skouboe, P., Taylor, J.W., Frisvad, J.C., Lauritsen, D., Larsen, L., Albaek, C., Boysen, M., Rossen, L., 2000. Molecular methods for differentiation of closely related *Penicillium* species. In: Samson, R.A., Pitt, J.I. (Eds.), Integration of Modern Taxonomic Methods for *Penicillium* and *Aspergillus* Classification. Harwood Academic Publishers, Netherlands, pp. 179–188.
Smith, N.J.H., 1980. Anthrosols and human carrying capacity in Amazonia. Ann. Assoc. Am. Geogr. 70, 553–556.
Sombroek, W., Ruivo, M.L., Fearnside, P.M., Glasser, B., Lehmann, J., 2003. Amazonian dark earths as carbon stores and sinks. In: Lehmann, J., Kern, D.C., Glaser, B., Woods, W.I. (Eds.), Amazonian Dark Earths: Origin, Properties, Management. Kluwer Academic Publishers, Dordrecht, pp. 125–139.
Steiner, C., Texeira, W.G., Zech, W., 2004. Slash and char: an alternative to slash and burn practiced in the basin. In: Glaser, B., Woods, W.I. (Eds.), Amazonian Dark Earths: Explorations in Space and Time. Springer, Berlin, pp. 183–193.
Suhas, Carrott P.J.M., Ribeiro, Carrott M.M.L., 2007. Lignin – from natural adsorbent to activated carbon: a review. Bioresour. Technol. 98, 2301–2312.
Takai, K., Oga, M., Sato, H., Enoki, T., Ohki, Y., Taomoto, A., Suenaga, K., Iijima, S., 2003. Structure and electronic properties of a nongraphitic disordered carbon system and its heat-treatment effects. Phys. Rev. B 67, 214202.
Talbot, J.M., Allison, S.D., Treseder, K.K., 2008. Decomposers in deguise: mycorrhizal fungi as regulators of soil C dynamics in ecosystems under global change. Funct. Ecol. 22, 955–963.
Tamura, K., Peterson, D., Peterson, N., Stecher, G., Nei, M., Kumar, S., 2011. MEGA5: molecular evolutionary genetics analysis using maximum likelihood, evolutionary distance, and maximum parsimony methods. Mol. Biol. Evol. 28, 2731–2739.
Vujanovic, V., Hamelin, R.C., Bernier, L., Vujanovic, G., St-Arnaud, M., 2007. Fungal diversity, dominance, and community structure in the rhizosphere of clonal *Picea mariana* plants throughout nursery production chronosequences. Microb. Ecol. 54, 672–684.
White, T.J., Bruns, T.D., Lee, S.B., 1990. Amplification and direct sequencing of fungal ribosomal RNA genes for phylogenetics. In: Innis, N.A., Gelfand, J., Sninsky, J., White, T. (Eds.), PCR Protocols: A Guide to Methods and Applications. Academic Press, San Diego, pp. 315–322.
Walker, C., Mize, W., McNabb, H.S., 1982. Populations of endogonaceus fungi at two populations in central Iowa. Can. J. Bot. 60, 2518–2529.
Zajac, J., Groszek, A.J., 1997. Adsorption of C60 fullerene from its toluene solutions on active carbons: application of flow microcalorimetry. Carbon 35, 1053–1060.